Jacques, S. D. M.; Leynaud, O.; Strusevich, D.; Beale, A. M.; Sankar, G.; Martin, C. M. and Barnes, P. (2006). Redox behavior of Fe-Mo-O catalysts studied by ultrarapid in situ diffraction. *Angewandte Chemie International Edition* **45** (3) 445-448.

New insights into redox behaviour of Fe-Mo-O catalysts as seen by ultra rapid *in situ* diffraction

Dr. S. Jacques*, Dr. O. Leynaud*, Mr. D. Strusevich*, Dr. A.M. Beale**, Prof. G. Sankar***, Dr. C.M. Martin****, Prof. P. Barnes*

* Industrial Materials Group, Materials Chemistry Centre, Department of Chemistry, University College London, 20 Gordon Street, London WC1H 0AJ, UK.
  Also: Department of Crystallography, Birkbeck College, Malet Street, London WC1E 7HX, UK.

** Department of Inorganic Chemistry and Catalysis, Sorbonnelaan 16, 3584 CA, Utrecht, The Netherlands.

*** The Royal Institution, 21 Albemarle Street, London W1X 4BS, UK.

**** CLRC Daresbury Laboratory, Daresbury, Warrington WA4 4AD, UK.

Suggested text for Table of Contents:
Hot air in a hurry: An industrial Fe-Mo-O catalyst has been studied under redox conditions using ultra rapid *in situ* diffraction. Surprisingly it is the oxidation step that is fastest, completing within 15 seconds at 472°C.

keywords: iron molybdate, in situ, X-ray diffraction, synchrotron, redox, rapid oxidation, catalysis

The term "Fe-Mo-O" is used to denote a mixed phase catalyst system as used, for example, in the production of formaldehyde which is an important building block molecule for complex chemicals in many consumer products. Almost all formaldehyde is manufactured by either: (i) dehydrogenation of a methanol-rich air mixture over a silver catalyst, or (ii) direct oxidation of methanol over a Fe-Mo-O based catalyst.[1,2a] The latter process is advantageous in that the exothermic reaction can be carried out at comparatively lower temperatures, typically 350°C, and the catalyst offers comparatively higher activity and selectivity.[2b] The mechanism is assumed to follow a Mars-van Krevelen like process of hydrocarbon oxidative dehydrogenation and this has been demonstrated for an industrial Fe-Cr-Mo-O preparation[3]. Methanol oxidation proceeds, as shown in equation (1), with a partial reduction of the active iron molybdate ($Fe_2(MoO_4)_3$) phase, followed by catalyst regeneration[4,5]:

$$CH_3OH + Fe_2(MoO_4)_3 \rightarrow 2(\beta\text{-}FeMoO_4) + MoO_3 + CH_2O + H_2O \quad (1)$$

There have been several notable studies on Fe-Mo-O catalysts[3,6-14] covering aspects of catalytic activity, deactivation and mechanism. In particular the Mo/Fe ratio is considered to be important; industrial preparations use a Mo/Fe ratio >1.5 comprising a mixture of two phases, $Fe_2(MoO_4)_3$ and MoO_3. It is thought that the primary function of MoO_3 is to provide a reservoir of molybdenum to balance losses through sublimation at reactor hot-spots which would otherwise prevent regeneration of the active phase and lead to the formation of Fe_2O_3 which favours total oxidation[1,7,15]. However, there have not been any previous diffraction studies which focus on the interplay between these phases and their effect on catalytic reaction and regeneration. Here we show the importance of observing these reactions using rapid time-resolved *in situ* powder diffraction; in particular we capture the responses of the Fe-Mo-O catalyst under accelerated aging conditions and show the importance of the *multiple-phase* form in maintaining catalyst longevity.

A special environmental cell system has been designed to apply redox cycling conditions to catalyst material while collecting (*in situ*) powder diffraction data on the synchrotron; this cell is illustrated in Figure 1 and described, with operational details, in the Experimental Section.

Figure 1: Schematic of the redox environmental cell consisting of a capillary furnace and gas delivery system. The incident and diffracted synchrotron X-ray beams are in a perpendicular plane (to the diagram), the exit window of the furnace spanning an angular range of 120°.

In order to confirm starting materials and basic methodology, diffraction patterns of the catalyst material, both as prepared and after reduction, were first analysed. The three component phases expected, $Fe_2(MoO_4)_3$, MoO_3, and $\beta\text{-}FeMoO_4$, account for all constituent peaks in the diffraction patterns once allowance is made for differential thermal expansion up to the operating temperature, 472°C: For $Fe_2(MoO_4)_3$, its two very similar allotropes[19] can be accommodated by using the high temperature form[20] extrapolated to 472°C; for MoO_3, in-house high temperature neutron data[21] were necessary to unravel the mixed (positive/negative) expansion contributions; for $\beta\text{-}FeMoO_4$, reliable data[22] could be found only for ambient conditions and so its 472°C diffraction peaks were identified by indexing the remaining peaks (*via* the Crysfire program[23]), using the ambient unit cell as a starting guide. The peak

positions of the three phases at 472°C were then all refined independently against the experimental patterns using the Celref program[24]. This provided an essential start set of parameters, as in Table 1, for the subsequent multi-phase Rietveld refinements of the *in situ* patterns obtained during redox cycles; no peaks remained unexplained, though there was residual intensity mismatch for some MoO_3 peaks during Rietveld refinement due to preferred orientation of MoO_3, typical of lamellar structures[21] (an example fit is given in the *Supporting Information*).

∞

Phase	Space Group	Unit cell parameters	Initial fraction	Reduced fraction
$Fe_2(MoO_4)_3$	P b c n	a = 12.88; b = 9.206; c = 9.323 Å	51 %	27 %
β-$FeMoO_4$	C 1 2/m 1	a = 10.36; b = 9.447; c = 7.107 Å; β = 106.4°	<1 %	19 %
MoO_3	P n m a	a = 14.20; b = 3.702; c = 3.989 Å	49 %	54 %

Table 1: Space groups, starting unit cell parameters and weight fractions for the three component phases, obtained by fitting simulated patterns to the diffraction patterns for the initial catalyst and the same after reduction at 472°C.

Figure 2a shows the time-resolved *in situ* patterns obtained during a reduction-oxidation-reduction cycle at 472°C. Here the collection time for each pattern was 30 seconds and the sequence covers 60 minutes spanning most of a complete cycle.

Figure 2: Contour images of *in situ* powder diffraction from a Fe-Mo-O catalyst at 472°C under successive reducing (→) and oxidising (→) atmospheres: (a) 120 × 30 s patterns showing the end of one reduction, a full oxidation and part of a second reduction stage; (b) an ultra-rapid acquisition (patterns every 2 seconds) illustrating the extreme rapidity of the oxidation stage.

The change in diffraction patterns on introduction of the oxidising gas (at 5 minutes) is dramatic, appearing to be discontinuous on the minutes timescale. By comparison, the changes during subsequent reduction (25-60 minutes) are far more gradual. The sequence of changes in peak positions is somewhat complicated by a small movement of the sample capillary in the diffractometer as the gas is changed: thus at 5 minutes there are peak shifts arising from both the structural changes and capillary movement whereas at 25 minutes the immediate shifts are entirely due to capillary movement. This effect has been effectively "subtracted out" in the subsequent data analysis. Multi-phase Rietveld structure refinement (cyclic mode of Fullprof[25] using WinPLOTR software[26]) has been performed over the 120 patterns shown in Figure3a in which the unit cells and scale factors (effectively molecular weight fractions) are allowed to vary but with the fractional atomic coordinates and the profile parameters kept fixed because of the unavoidable preferred orientation effects mentioned previously. The resulting variations in weight fraction *versus* time are given in Figure3a; the general trends are clear over and above the irregularities (e.g. ~50 min.) which arise from inhomogeneities in gas flow/penetration through the large specimen agglomerates required to pack the capillary (see Experimental Section). The *Supporting Information* shows that these irregularities can be smoothed-out by using larger specimen capillaries (4 mm diam.) but at the expense of data speed/resolution which is required for the oxidation stage (see later).

Figure 3: Phase composition (% mol weight fractions) of $Fe_2(MoO_4)_3$, β-$FeMoO_4$ and MoO_3 obtained by multiphase Rietveld fitting to the data shown in Figure 3 (same gas environment notation):
(a) variations on the minutes timescale showing incomplete reduction even after 36 minutes;
(b) capturing the rapid oxidation stage on a seconds timescale.

The disproportionate rapidity of the oxidation stage, compared to reduction, required that it be re-examined while pushing the system performance to its limit. The result is Figure 2b which shows the oxidation stage captured in 2 second diffraction intervals. In order to quantify this further, multi-phase-Rietveld refinements were performed on the 2 second diffraction patterns spanning the transition. The resulting scatter is unavoidably increased, nevertheless the time-profile obtained (Figure 3b) clearly shows the progression of this transition and that the oxidation reactions are virtually completed within 15 seconds. At present one can only speculate on why there should be such a huge difference in the reduction and oxidation rates: Firstly one notes that the standard redox potential, +0.77 V, for $Fe^{3+} + e^- \rightarrow Fe^{2+}$ rather suggests a favoured reduction (forward direction) though one should also consider the observation[14] that this might occur via a two step process at the catalyst surface, first Mo^{6+} to Mo^{5+} before Fe^{3+} to Fe^{2+}. Other explanations relating to higher oxygen anion mobilities for the β-$FeMoO_4$ phase, to aid solid state transport of oxygen during oxidation, remain questionable in light of the rapid oxidation rates observed. A more intriguing possibility, for which there is some supporting evidence[27],[28], concerns the physico-chemical nature of the reduction reaction itself (see equation (2)), whereby H_2O production will block access of hydrogen to the Fe-Mo-O active sites during reduction; by contrast, known rapid oxygen uptake[29] clearly aids the re-oxidation process. Importantly, one also notes that the presence of other crystalline Mo/Fe reduced phases are clearly ruled out by the diffraction data.

In conclusion, this study has demonstrated the power of ultra rapid *in situ* powder diffraction for obtaining new insights into the high temperature solid-state redox processes occurring in a mixed catalyst system; the combination of intense synchrotron wiggler radiation, X-ray optics and an ultra-rapid/high resolution detector enables one to follow both slow reactions and those that are too fast for capture by conventional laboratory or synchrotron techniques. It is possible to rationalise the behaviour according to a Mars-van Krevlen type process: in a 5% H_2/Ar atmosphere the $Fe_2(MoO_4)_3$ phase undergoes reduction according to equation (2) and subsequent regeneration in 5% O_2/Ar according to equation (3),

$$H_2 + Fe_2(MoO_4)_3 \rightarrow 2(\beta\text{-}FeMoO_4) + MoO_3 + H_2O \quad (2)$$

$$2(\beta\text{-}FeMoO_4) + MoO_3 + \tfrac{1}{2}O_2 \rightarrow Fe_2(MoO_4)_3 \quad\quad (3),$$

The speed of the redox processes at 472°C has been uniquely determined: Even though these are multi-phase solid state reactions the oxidation stage is found to be extremely fast; at 472°C oxidation is effectively completed within 15 seconds in contrast to the reduction stage which is incomplete even after 36 minutes. This appears contrary to existing viewpoint (e.g. Pernicone[12]) that reduction of $Fe_2(MoO_4)_3$ is easier than oxidation of β-$FeMoO_4$. This difference in reactivity will be critical for maintaining phase stability and catalyst activity. The absence of any additional phases suggests that reaction (3) proceeds so quickly that other solid-state side reactions leading to deactivation (e.g. equation 4) are avoided:

4

$$2(\beta\text{-FeMoO}_4) + \tfrac{1}{2}O_2 \rightarrow Fe_2O_3 + 2MoO_3 \qquad (4)$$
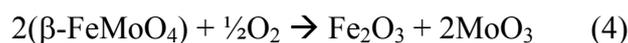
Therefore we demonstrate that adding an excess of MoO_3 in the as-prepared catalyst is beneficial for maintaining the stability of the active phase as well as replenishing any sublimed molybdenum that might occur. Finally we note that although there have been previous attempts to capture redox processes occurring in single phase systems this is the first diffraction study, as far as the authors are aware, of such rapid reactions within a mixed phase solid state system. Many other catalytic systems can now realistically become candidates for detailed study by this method, including optimisation of catalyst composition and working temperature.

Experimental Section

The industrial-like iron molybdate catalyst was prepared with an Mo/Fe atomic ratio of 3:1 using a co-precipitation method similar to that by Soares *et al.* [6] using appropriate amounts of $(NH_4)_6Mo_7O_{24}.4H_2O$ and $Fe(NO_3)_3.9H_2O$. The product was calcined at 375°C for 2 hours and then pelletised, crushed and coarsely sieved to obtain suitable agglomerates for mounting inside the furnace quartz capillary.

The environmental cell system consists primarily of a capillary furnace and gas delivery system (Figure 1). The furnace is sufficiently small (100 mm diam., 47 mm height) to facilitate connection of the capillary to a gas inlet/outlet. A thermocouple adjacent to the sample regulates the temperature, the recorded temperatures being corrected by means of prior calibrations with a probable error of ±10°C, which is confirmed by the subsequent regression analysis of the high temperature MoO_3 unit cell dimensions. Inert (100% Ar), reducing (5% H_2/Ar) and oxidising (5% O_2/Ar) gases can be passed through the heated sample capillary during data collection, with remote start/stop control. The sample, contained in the 1mm diameter quartz capillary, is protected from loss into the flowing gas by quartz wool plugs.

All data collection was carried out on station 6.2 of the SRS synchrotron (Daresbury, UK). This station has been recently commissioned[16,17] as a high flux multipole wiggler beamline facility for materials processing. In powder diffraction mode, the optics system delivers an incident X-ray footprint of 0.5mm×3mm for capillary operation, the selected incident wavelength being 1.400 Å. Diffraction data were collected using the *RAPID2* detector[16] which realises a medium-high angular resolution (0.06°) at ultra-high count-rates (20 MHz global) through its multi-wire/multi-electronic-channel mode of operation, over a nominal 2θ-range of 60°. The resulting rapid powder diffraction patterns are of sufficient quality for Rietveld[18] structure refinement.

References

[1] B. Stiles, T. A. Koch, *Catalyst Manufacturer*, 2nd Ed, Marcel Dekker, New York, **1995**,. 197.

[2] a) R. Crichton, *Informally Speaking, The Formaldehyde Newsletter from Perstorp Formox,* Claes Lundström, Perstorp Formox AB, SE-284 80 Perstorp, Sweden (or http://www.perstorpformox.com.), **2003**, Spring/Summer, pp. 12-13; b) A Andersson, *ibid*, **2003**, Autumn/Winter, pp. 10-12.

[3] D. S. Lafyatis, G. Creten, G. F. Froment, *Appl. Catal. A* **1994**, 120, 85-103.

[4] A. V. Demidov, I. G. Danilova, G. N. Kustova, L. M. Plyasova, N. G. Skomorokhova, L. L Sedova, V. B. Nakrokhin, B. I. Popov, *Kinetics & Catal.* **1992**, 33, 910-914.

[5] G. Alessanadrini, L. Cairati, P. Forzatti, P. L. Villa, F. Trifirò, *J. Less Common Metals* **1977**, 54, 373-386.

[6] A. P. V. Soares, M. Farinha Portela, A. Kiennemann, L. Hilaire, J. M. M Millet, *Appl. Catalysis. A* **2001,** 206, 221-229.

[7] A. P. V. Soares, M. Farinha Portela, A. Kiennemann, *Catal. Commun.* **2001**, 2, 159-164.

[8] A. P. V. Soares, M. Farinha Portela, A. Kiennemann, L. Hilaire, *Chem. Eng. Sci.* **2003**, 58, 1315-1322.

[9] J-L. Li, Y-X. Zhang, C-W. Liu, Q-M. Zhu, *Catal. Today* **1999**, 51, 195-199.

[10] J. H. Wilson III, C. G. Hill Jr., J. A. Dumesic, *J. Molec. Catal.* **1990**, 61, 333-352.

[11] C. J. Machiels, W. H. Cheng, U. Chowdhry, W. E. Farneth, F. Hong, E. M. McCarron, A. W. Sleight, *Appl. Catal.* **1986**, 25, 249-256.

[12] N. Pernicone, *Catal. Today* **1991**, 11, 85-91.

[13] V. Diakov, D. Lafarga, A. Varma, *Catal. Today* **2001**, 67, 159-167.

[14] H. Zhang, J. Shen, X. Ge, *J. Solid State Chem.* **1995**, 117, 127-135.

[15] M. Bowker, R. Holroyd, A. Elliott, P. Morrall, A. Alouche, C. Entwistle, A. Toerncrona, *Catalysis Lett.* **2002**, 83, 165-176.

[16] A. Berry, W. I. Helsby, B. T. Parker, C. J. Hall, P. A. Buksh, A. Hill, N. Clague, M. Hillon, G. Corbett, P. Clifford, A. Tidbury, R. A. Lewis, R. J. Cernik, P. Barnes, G. E. Derbyshire, *Nucl. Instr. & Meth. Phys. Res.* A **2003**, 513**,** 260–263.

[17] R. J. Cernik, P. Barnes, G. Bushnell-Wye, A. J. Dent, G. P. Diakun, J. V. Flaherty, G. N. Greaves, E. L. Heeley, W. Helsby, S. D. M. Jacques, J. Kay, T. Rayment, A. Ryan, C. C. Tang, N. J. Terrill, *J. Synchrotron Rad.* **2004**, 11, 163-170.

[18] H. M. Rietveld, *J. Appl. Cryst.* **1969**, 2, 65-71.

[19] A. W. Sleight, L. H. Brixner, *J. Solid State Chem.* **1973**, 7, 172-174.

[20] W. T. A. Harrison, *Mater. Res. Bull.* **1995**, 30, 1325-1331.

[21] E. Lalik, *PhD thesis*, University of London (UK) **2003**.

[22] A. W. Sleight, B. L. Chamberland, J. F. Weiher, *Inorg. Chem.* **1968**, **7**, 1093-1098.

[23] Shirley, R. The CRYSFIRE System for Automatic Powder Indexing: User's Manual (The Lattice Press, Surrey GU2 5NL, UK), **1999**.

[24] J. Laugier, B. Bochu, Celref software, part of the LMGP Suite using the GETSPEC software referred to by: U. D. Altermatt, I. D. Brown, *Acta Cryst. A* **1987**, 43, 125-130.

[25] J. Rodriguez-Carvajal, FULLPROF: A Program for Rietveld Refinement and Pattern Matching Analysis, *Abstr. Satellite Meeting Powder Diffraction, XV Congr. It. Union Cryst.*, **1990**, 127.

[26] T. Roisnel, J. Rodríguez-Carvajal, WinPLOTR: a Windows tool for powder diffraction patterns analysis, *Mater. Sc. Forum* **2001**, 378, 118-123.

[27] N. Pernicone, F. Lazzerin, G. Lanzvecchia, *J. Catalysis*, **1968**, 10, 83.
[28] A. P. V. Soares, M. F. Portela, A. Klennemann, *Catalysis Rev.,* **2004**, 47, 125-174.
[29] K Otsuka, Y Wang, *Appl. Catalysis*, **2001**, 222, 145-161.

Capillary with sample

Furnace

Heater Cage

Solenoid Switches (controlled from outside the experimental area)

Ar 95% + H₂ 5%

Ar 99.9%

Ar 95% + O₂ 5%

Gas Cylinders